



Decarbonylation of water insoluble carboxaldehydes in aqueous microemulsions by some sol–gel entrapped catalysts



Shirel Dahoah^a, Zackaria Nairoukh^a, Monzer Fanun^b, Michael Schwarze^c, Reinhard Schomäcker^c, Jochanan Blum^{a,*}

^a Institute of Chemistry, The Hebrew University, Jerusalem 91904, Israel

^b Center for Colloid and Surface Research, Al-Quds University, East Jerusalem 51000, Palestinian Authority

^c Institut für Chemie, Technische Universität Berlin, Strasse des 17. Juni 124, D-10623 Berlin, Germany

ARTICLE INFO

Article history:

Received 7 August 2013

Received in revised form

16 September 2013

Accepted 17 September 2013

Available online 26 September 2013

Keywords:

Aldehyde decarbonylation

Heterogeneous catalysis

Microemulsion

Palladium nanoparticles

Sustainable chemistry

ABSTRACT

In the course of our attempts to replace harmful solvents in organic processes by environmentally favored media, we investigated the use of aqueous microemulsions for catalytic decarbonylation of different kinds of aldehydes. The aldehydes were solubilized in the microemulsions with the aid of the cationic surfactant, cetyltrimethylammonium bromide. The aldehydes were transferred into CO-free products by sol–gel entrapped catalysts. The best results were obtained in the presence of nanoparticles of Pd(0). The heterogenized catalyst could usually be recycled 7–8 times without loss of catalytic activity. At relatively low temperatures (140 °C) the decarbonylation proceeds stepwise. Initially a mixture of saturated and unsaturated products is formed. At 180 °C however, fast hydrogenation of the unsaturated compounds takes place. These investigations may be regarded as model studies for the conversion of biomass derived intermediates to fuels and chemicals.

© 2013 Elsevier B.V. All rights reserved.

1. Introduction

With the intention to reduce the amount of harmful organic solvents used in many synthetic and catalytic processes through their replacement by water we have already developed a general system in which the substrates are solubilized in aqueous emulsions and the catalysts can be recycled [1]. In these systems suitable surfactants promote the solubilization in the aqueous media and sol–gel materials support the catalysts. So far, we found that our system can be applied to a variety of hydrogenations processes [1], transfer hydrogenation [2], regioselective hydroformylation [3], double bond migration in allylic compounds [4], disproportionation of dihydroarenes [5], carbon–carbon bond coupling processes [6,7] (Heck, Suzuki, Stille and multi-component addition reactions). We now find that the combination of aqueous emulsions of the substrates and sol–gel entrapped catalysts – the so-called emulsion/solid-heterogenization method for transport and catalysis (EST) – is applicable to facile aldehyde decarbonylation processes. Under conventional conditions (i.e., in organic solvents) aldehyde decarbonylations are involved in a variety of both industrial and academic studies (for some recent reviews see

e.g., Refs. [8–10]). The decarbonylation takes place in the presence of either transition metal derived catalysts [8], by a variety of enzymes [11] or under photochemical conditions [12]. The key step in the transformation of biomass into fuels is often assumed to involve decarbonylation of the degradation products of plants and animals, and some of the natural pathways have been imitated [13]. The facile deformylation of aldehydes enables the utilization of carboxaldehydes for gas-free carbonylation and for transfer hydrogenation [14]. The use of an aqueous medium in aldehyde decarbonylations by a recyclable catalyst can be regarded as a green version of this important process and mimics the suggested route to hydrocarbon fuels [13].

2. Experimental

2.1. Instruments

NMR spectra were recorded on a Bruker DRX-400 instrument in CDCl₃. Infrared spectra were obtained with a Perkin-Elmer 65 FTIR spectrometer. Mass spectral measurements were performed with a Q-TOF-II spectrometer. ICP-MS analyses were carried out with a Perkin-Elmer model DRC II instrument. A Quantachrome Novawin Instrument version 10.01 was used for Brunner, Emmet, Teller (BET-N₂) and Barett, Joyner, Halenda (BJH-N₂) surface area and pore diameter measurements of the sol–gel matrices. Gas

* Corresponding author. Tel.: +972 2 6585329; fax: +972 2 6513832.

E-mail address: jochanan.blum@mail.huji.ac.il (J. Blum).

chromatographic determinations were carried out with a Hewlett-Packard model Agilent 4890D by using either a 30 m long column packed with Carbowax 20M-poly(ethylene glycol) in fused silica (Supelco 25301-U) or a 15 m long column packed with bonded and crosslinked (5% phenyl)methyl polysiloxane (HP-5). X-ray Photoelectron Spectroscopy (XPS) measurements were performed on a Kratos Axis Ultra X-ray photoelectron spectrometer (Karatos Analytical Ltd., Manchester, UK). High resolution XPS spectra were acquired with monochromatic AlK α X-ray radiation source (1486.6 eV) with 90° takeoff angle (normal to the analyzer). The pressure in the chamber was about 2×10^{-9} Torr. The wide (survey) spectra were obtained for range 0–600 eV with pass energy 150 eV and step 1 eV. The high-resolution XPS spectra were collected for C 1s, Si 2p and Pd 3d levels with pass energy 20 eV and step 0.1 eV. The binding energies (BE) were calibrated respecting to the C1s peak energy position as 285.0 eV. Data analyses were performed using Casa XPS (Casa Software Ltd.) and Vision data processing program (Kratos Analytical Ltd.). Transmission electron microscopy (TEM) was done with a scanning transmission microscope Technai G² F20 operated at 200 kV and equipped with an EDAX-EDS device for identification of the elemental composition. Initial powders were dispersed in ethanol and dropped onto a standard 400 mesh carbon coated copper TEM grid.

2.2. Chemicals

The unsubstituted benzaldehyde, 2- and 4-chlorobenzaldehyde, 4-methyl-, 4-methoxy-, and 4-ethylbenzaldehyde, 1-naphthaldehyde, 3-phenylpropionaldehyde, 3-phenylbutyraldehyde, *E*-cinnamaldehyde, 1-decanal, as well as all the reference compounds (CO-free hydrocarbons), and the surfactant cetyltrimethylammonium bromide, the sol-gel precursor tetramethoxysilane, the precursors of the catalysts, palladium acetate, disodium tetrachloropalladate trihydrate, rhodium and iridium trichloride hydrates, 3-aminopropyltrimethoxysilane, 2,5-di-*tert*-butylhydroquinone, 1,2-(diphenylphosphinopropane) (dppp) and sodium borohydride were obtained from commercial sources. 2-Phenylpropionaldehyde [8] as well as bis[1,3-bis(diphenylphosphino)-propane]rhodium chloride [15] were prepared according to literature processes.

2.3. Preparation and entrapment of metallic nanoparticles in sol-gel matrices

Metallic nanoparticles were prepared by the method of Bharath et al. [16]. Typically, to a solution of Na₂PdCl₄·3H₂O (30 mg, 0.086 mmol) and H₂NCH₂CH₂CH₂Si(OMe)₃ (0.8 ml) in MeOH (27 ml) was added under N₂ at room temperature solid NaBH₄ (27 mg) essentially as previously described [17]. After stirring the mixture for 15 h the MeOH was removed by decantation and to the residue was added THF (2 ml), triply distilled water (TDW, 2 ml) and TMOS (3.6 ml). The stirring was continued as long as possible. The gel was washed and sonicated with ether (2 × 20 ml) dried at 80 °C and 0.5 Torr to obtain constant weight. By this procedure we usually obtained 1.4–1.6 g of sol-gel entrapped Pd(0) nanoparticles.

Sol-gel entrapped Rh(0) and Ir(0) nanoparticles were obtained by the same methods from the corresponding metal trichloride hydrates.

The surface area and pore-diameters of matrices of selected entrapped catalysts have been measured.

2.4. Preparation of the microemulsions of the aldehydes

A mixture of freshly distilled aldehyde (1 mmol which amounts to ca. 0.8 wt.% of the expected microemulsion), TDW (15–20 ml, 90.1 wt.%), cetyltrimethylammonium bromide (CTAB, 0.4–0.8 g, ca.

2.5 wt.%) and 1-propanol (1.2 ml, 6.6 wt.%) was stirrer magnetically at room temperature (25 °C) until a clear transparent mixture that scatters laser beams was formed. In some cases the addition of a few drops of 1-propanol was necessary.

2.5. General procedure for the catalytic decarbonylation process

The sol-gel entrapped catalyst (10–200 mg) was roughly ground and placed together with 2,5-di-*tert*-butylhydroquinone (10 mg) and a freshly prepared microemulsion of an aldehyde in a mini autoclave equipped with a sampler through which small samples could be removed periodically. The reaction mixture was purged with nitrogen, stirred magnetically and heated with a controllable thermostat at the required temperature for the desired length of time. The reaction mixture was cooled to 20 °C. For the determining of the evolved CO the gases were transferred to a toluene solution of excessive ClRh(PPh₃)₃. The transformation of the latter complex to ClRh(CO)(PPh₃)₃ started immediately. After 1 h the rhodium carbonyl complex was filtered, dried and analyzed. In all experiments the amount of the isolated rhodium carbonyl complex was above 78%. The used sol-gel entrapped catalyst was filtered off from the reaction mixture, and the filtrate was separated from the oily layer by addition of an excess of NaCl. Sometimes the microemulsions underwent spontaneous separation into two phases without addition of the salt. The aqueous phase was extracted with either hexane or ether and analyzed by comparison with authentic samples. The used catalyst was washed and sonicated with water and ether prior to its use in further catalytic runs.

3. Results and discussion

Some examples of catalytic decarbonylation of 3-phenylpropionaldehyde by sol-gel engaged rhodium, iridium and palladium derivatives are summarized in Table 1. Further decarbonylations that have been studied are shown in Scheme 1.

Upon completion of the decarbonylation process metallic nanoparticles were found within the sol-gel matrices even when the initial heterogenized catalyst was nanoparticle-free organometallic complexes. An example of such nanoparticles generated from sol-gel engaged ClRh(PPh₃)₃ during decarbonylation of 3-phenylpropionaldehyde are shown in the TEM-micrograph in Fig. 1. Whether the immobilized metallic nanoparticles or the residual complexes are responsible for the catalytic processes could not be estimated at this stage of our research. At 140 °C the phenylpropanals underwent decarbonylation and dehydrogenation to ethylbenzene and styrene by the catalysts (except by the iridium compound, Table 1, entry 6). The ratio between the two products changes however, by the introduction of minor alterations of the reaction conditions. At higher temperatures (>180 °C) the styrene,

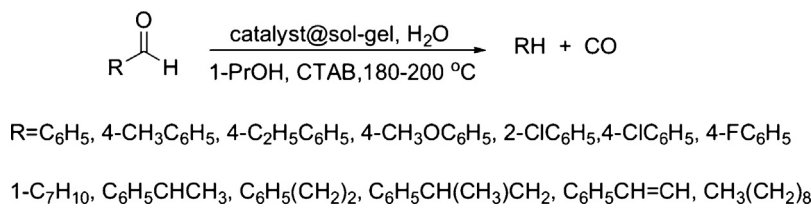
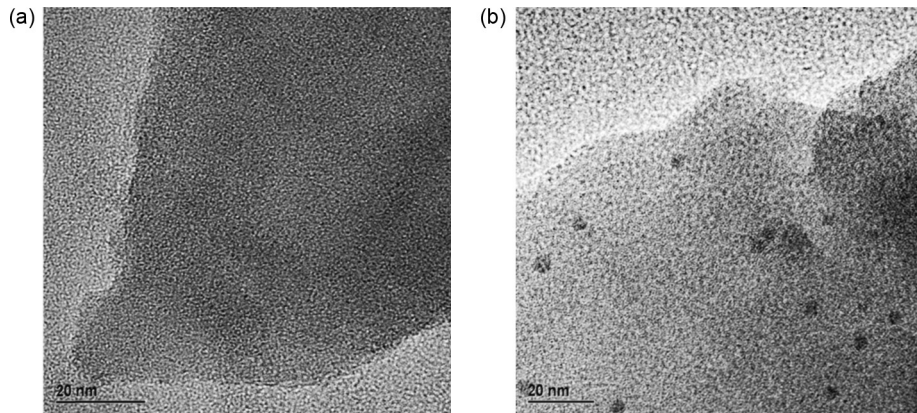
Table 1

Decarbonylation of 3-phenylpropanal to ethylbenzene by some sol-gel entrapped transition metal catalysts under EST conditions.^a

Entry	Catalyst	Conversion of substrates, ^b %
1	Rh(0)@sol-gel	5
2	RhCl(PPh ₃) ₃ @sol-gel	13
3	RhCl(dppp) ₂ @sol-gel	20
4	Pd(0)@sol-gel	70.5
5	Pd(OAc) ₂ @sol-gel	14
6	Ir(0)@sol-gel	44

^a Reaction conditions: precatalyst (0.1 mmol) engaged within sol-gel from TMOS (3.6 ml), water (15 ml), 1-propanol (1.1 ml), cetyltrimethylammonium bromide (400 mg), 140 °C, 24 h. The percentage of water of the microemulsion was ~90 wt.%.

^b These figures represent the total yield of ethylbenzene (decarbonylation product) and of styrene (dehydrodecarbonylation) except for entry 6.

**Scheme 1.** Decarbonylation of carboxaldehydes.**Fig. 1.** TEM images of sol-gel entrapped $\text{ClRh}(\text{PPh}_3)_3$ (a) before and (b) after decarbonylation of 3-phenylpropionaldehyde.

in the presence of 2,5-di-*tert*-butylhydroquinone, undergoes fast transfer hydrogenation to ethylbenzenes.

The metallic pre-catalysts were prepared simply by $\text{H}_2\text{N}(\text{CH}_2)_3\text{Si}(\text{OMe})_3\text{-NaBH}_4$ reduction of the corresponding metal chlorides in analogy to the method of Bharath et al. [16]. Their entrapment within the silica sol-gel matrices was performed as previously reported [17]. Their BET- N_2 and BJH- N_2 analyses revealed high surface areas before the decarbonylation processes, which changed, however, during the catalytic reactions (vide infra). The immobilized catalyst proved to be an efficient decarbonylation catalyst for a variety of aldehydes. Except for compounds **4**, **5**, **7**, **10** and **13**, the aldehydes listed in Table 2 were transferred completely into the respective carbonyl-free products

in quantitative yields by heating them either for 22 h at 200 °C or for 45 h at 180 °C in aqueous microemulsions. The aforementioned aldehydes gave lower yields either because of steric effects (cf. entries 5 and 6) or because of electronic reasons (compare entries 4 and 6). We do not fully understand the diminished activity of the fluorinated compound **7**. We assume that the formations of some stable complexes with the fluorine moiety are formed. The yields of decarbonylation of compounds **4**, **5**, **7**, **11** and **13** after 45 h at 180 °C were 47, 71, 44, 50 and 22%, respectively. Some comparative aldehyde decarbonylations for 5 h at 180 °C are summarized in Table 2. The further progress of the reaction at extended reaction time shows that the catalyst is not deactivated by the substrates **4**, **5**, **7**, **11** and **13**. The yields of the decarbonylation products were determined, in addition to conventional GC and NMR analyses, also by transferring the evolved gases into a toluene solution of $\text{ClRh}(\text{PPh}_3)_3$ that gives in the presence of the CO, the sparingly soluble $E\text{-ClRh}(\text{CO})(\text{PPh}_3)_3$. Kinetic measurements revealed that under the EST conditions all the decarbonylations studied follow the first order rate law in the substrate but only some of them can be expressed in terms of a Hammett plot (see Table 3 and Fig. 2). Thus, the decarbonylations in aqueous microemulsions resemble the features of the reactions in diglymes [18,19]. In both systems the Hammett plots have positive slopes, which suggest that electron-attracting groups enhance the reaction and electron withdrawing ones cause the decarbonylation to slow down. The effect in the aqueous medium ($\rho = 1.65$) surpasses that in the

Table 2

Decarbonylation of some aldehydes by sol-gel encaged Pd(0) particles under comparable reaction conditions.^a

Entry	Substrates	Main product ^b (conversion, %)
1	Benzaldehyde (1)	Benzene (60)
2	4-Tolualdehyde (2)	Toluene (42)
3	4-Ethylbenzaldehyde (3)	Ethylbenzene (67)
4	4-Methoxybenzaldehyde (4)	Anisole (15)
5	2-Chlorobenzaldehyde (5)	Chlorobenzene (3)
6	4-Chlorobenzaldehyde (6)	Chlorobenzene (85)
7	4-Fluorobenzaldehyde (7)	Fluorobenzene (11)
8	1-Naphthaldehyde (8)	Naphthalene (66)
9	2-Phenylpropionaldehyde (9)	Ethylbenzene (99)
10	3-Phenylpropionaldehyde (10)	Ethylbenzene (10) ^c
11	3-Phenylbutyraldehyde (11)	Cumene (10) ^d
12	E-Cinnamaldehyde (12)	Styrene (9)
13	1-Decanal (13)	Nonane (4)

^a Typical reaction conditions: sol-gel entrapped Pd(0) nanoparticles (0.086 mmol, roughly ground); microemulsion of aldehyde (1 mmol, ~0.8–1.0 wt.%), CTAB (2.5 wt.%), 1-PrOH (6.6 wt.%), TDW (90.1 wt. %); 180 °C, 5 h within a glass lined autoclave. The products were analyzed by comparison with standard solutions of authentic samples of the corresponding saturated and unsaturated products.

^b The conversions are the average of at least two experiments that did not differ by more than ±3%.

^c Accompanied by 7% styrene.

^d Accompanied by 5% isopropenylbenzene.

Table 3

Substituent effect on the catalytic decarbonylation of some benzaldehydes by heterogenized Pd(0) nanoparticles under the EST conditions.^a

Entry	Substrate	k [10 ⁻⁵ ms ⁻¹]	k_s/k_a	$\log(k_s/k_a)$ ^b
1	4-H ₃ CO ₆ H ₄ CHO	1.30	0.26	-0.588
2	4-H ₃ CC ₆ H ₄ CHO	3.00	0.58	-0.236
3	C ₆ H ₅ CHO	5.17	1.00	0
4	4-ClC ₆ H ₄ CHO	9.67	1.87	0.272

^a Reaction conditions as in Table 2.

^b k_a and k_s represent the reaction constants for the composition of the unsubstituted and substituted benzaldehyde, respectively.

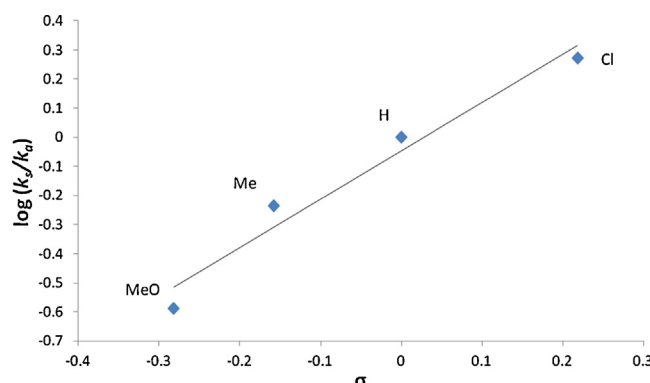


Fig. 2. Hammett plot for the decarbonylation of some benzaldehyde derivatives using sol-gel encaged Pd(0) nanoparticles at 180 °C as catalyst. The σ values were taken from Ref. [19]; $Y = 1.65$; $R^2 = 0.9631$.

organic solvent. The fact that metallic palladium particles promote the decarbonylation could suggest that during the process the metallic nanoparticles are transformed into a catalytically active complex (as e.g., in the arene hydrogenation process) by the nanoparticle formed from $\text{Rh}_2\text{Co}_2(\text{CO})_{12}$ [20,21]. However, we were unable to trace by IR any metal-carbonyl bands that may confirm this suggestion. Furthermore, XPS studies on the oxidation state of the palladium after the decarbonylation process indicate only the presence of Pd(0) species. In the high resolution spectrum in the 300–346 eV range appeared a sharp peak of Pd 3d_{5/2} on 335.5 eV and of Pd 3d_{3/2} on 340.7 eV which corresponds to Pd(0) [22].

As indicated above the BET-N₂ and BJH-N₂ analyses of the sol-gel matrices in which the metallic nanoparticles were entrapped, reveal structural changes during the decarbonylation processes. While the average surface area of the Pd(0) particle loaded sol-gel materials was 559 m²/g before the decarbonylation and the pore diameter 33 nm, the surface area decreased to 215–255 m²/g after the reactions. But no change in the pore volumes was detected. We recall that in other cases where sol-gel entrapped palladium catalyst was applied (e.g., in the catalytic Heck coupling [6]) the surface area decreased upon recycling of the immobilized catalyst owing to the Si–O bond cleavage by hydrolysis during the catalysis in the aqueous media. The recyclability of the Pd(0) particles was found to be unusually high, in most cases no decrease in the rate could be observed. In a typical series of experiments of decarbonylation of 4-chlorobenzaldehyde for 18 h at 180 °C the yields were 96–100% for the first 7 runs. Only at the eighth run the yield dropped sharply to 76%.

4. Conclusions

The EST system is applicable to the decarbonylation of a variety of aldehydes in aqueous media. During the decarbonylation the immobilized catalysts form metallic nanoparticles that can be recycled at least seven times without loss of catalytic activity. The most efficient catalyst studied is the one derived from palladium nanoparticles. At 140 °C the decarbonylations lead in part to the formation of alkenes. At 180–200 °C the saturated alkane derivatives are the predominate products.

Acknowledgement

We gratefully acknowledge the financial support of this trilateral study by the Deutsche Forschungsgemeinschaft (DFG) through grant SCHO687/8-2. We also thank Dr. Inna Popov for her help in the TEM studies, Dr. Vitaly Gutkin for his help in the XPS work and Gilad Zafirri for the BET and NJH measurements.

References

- [1] R. Abu-Reiq, D. Avnir, J. Blum, *Angew. Chem. Int. Ed.* **41** (2002) 423–426.
- [2] C. Batarseh, Z. Nairoukh, I. Volovich, M. Schwarze, R. Schomäcker, M. Fanun, J. Blum, *J. Mol. Catal. A: Chem.* **366** (2013) 210–214.
- [3] Z. Nairoukh, J. Blum, *J. Mol. Catal. A: Chem.* **358** (2012) 129–133.
- [4] D. Melzer, D. Avnir, M. Fanun, V. Gutkin, I. Popov, R. Schomäcker, M. Schwarze, J. Blum, *J. Mol. Catal. A: Chem.* **335** (2011) 8–13.
- [5] T. Yosef, R. Schomäcker, M. Schwarze, M. Fanun, F. Gelman, J. Blum, *J. Mol. Catal. A: Chem.* **351** (2011) 46–51.
- [6] T. Tsvelikhovsky, J. Blum, *Eur. J. Org. Chem.* (2008) 2417–2422.
- [7] H. Nowothnick, J. Blum, R. Schomäcker, *Angew. Chem. Int. Ed.* **50** (2011) 1918–1921.
- [8] J. Tsuji, in: E.-I. Negishi (Ed.), *Handbook of Organopalladium Chemistry for Organic Synthesis*, vol. 2, Wiley, New York, 2002, pp. 2643–2653.
- [9] M.A. Garralda, *Dalton Trans.* (2009) 3635–3645 (and references cited therein).
- [10] A. Koroticka, D. Necas, M. Kotora, *Curr. Org. Chem.* **16** (2012) 1170–1214.
- [11] D. Dar, E.H. Bekir, J.-H. Han, A. Sciore, E.N.G. Marsh, *Angew. Chem. Int. Ed.* **50** (2011) 7148–7152;
- [12] D. Dar, E.H. Bekir, J.-H. Han, A. Sciore, E.N.G. Marsh, *Angew. Chem. Int. Ed.* **51** (2012) 7881.
- [13] W.M. Horfspool, *Photochemistry* **32** (2001) 49–73.
- [14] M.O. Miranda, A. Pietrangelo, M.A. Hillmyer, W.B. Tolman, *Green Chem.* **14** (2012) 490–494.
- [15] T. Morimoto, M. Fujioka, K. Fuji, K. Tsutsumi, K. Kakiuchi, *Pure Appl. Chem.* **80** (2008) 1079–1087.
- [16] D.M. Doughty, L.H. Pignolet, *J. Am. Chem. Soc.* **100** (1978) 7083–7085.
- [17] S. Bharath, N. Fishelson, O. Lev, *Langmuir* **15** (1999) 1929–1937.
- [18] R. Abu-Reiq, D. Avnir, I. Miloslavski, H. Schumann, J. Blum, *J. Mol. Catal. A: Chem.* **185** (2002) 179–185.
- [19] P. Fristrup, M. Kreis, A. Palmeland, P.-O. Norby, R. Madsen, *J. Am. Chem. Soc.* **130** (2008) 5206–5215.
- [20] T. Matsui, H.C. Ko, G. Hepler, *Can. J. Chem.* **52** (1974) 2906–2911.
- [21] D. Evans, J.A. Osborn, G. Wilkinson, *Inorg. Chem.* **28** (1990) 79–80.
- [22] F. Gelman, D. Avnir, H. Schumann, J. Blum, *J. Mol. Catal. A: Chem.* **171** (2001) 191–194.